International Journal of GEOMATE, Sept. 2022, Vol.23, Issue 97, pp.74-81
ISSN: 2186-2982 (P), 2186-2990 (O), Japan, DOI: https://doi.org/10.21660/2022.97.3117
Geotechnique, Construction Materials, and Environment

INFLUENCES OF GRINDING PROCESS ON THE PHYSICAL AND MORPHOLOGICAL CHARACTERISTICS OF ULTRAFINE TREATED RICE HUSK ASH

*Siti Asmahani Saad[1], Aida Nabila Jamaluddin[1], Siti Aliyyah Masjuki[1], Salmia Beddu[3] and Nasir Shafiq[2]

[1]Faculty of Engineering, International Islamic University Malaysia, Malaysia; [2]Faculty of Engineering, University of Technology PETRONAS, Malaysia; [3]College of Engineering, University Tenaga Nasional, Malaysia

*Corresponding Author, Received: 01 March 2022, Revised: 13 June 2022, Accepted: 02 Aug. 2022

ABSTRACT: This paper aims to extend the investigation of producing highly reactive additive material in ultrafine size, with a particle diameter of less than 5μm through mechanical activation using a planetary ball mill. In light of the mechanical activation process, most studies were done to test materials such as metakaolin and fly ash. However, studies on the mechanical activation effect via planetary ball mill to conventional RHA or treated RHA are limited. In this research, raw rice husk (RH) was treated using a low heated concentration of acid, i.e., 0.01 - 0.1M hydrochloric acid (HCl). Then, the treated RH was combusted at 600 - 800°C. Finally, the treated RHA was ground using a planetary ball mill for 15 - 60 minutes. As a result, it was also observed that a burning temperature of 600°C, treated at four hours and ground at 300rpm for 15 minutes, had the finest size of ultrafine treated RHA (UFTRHA) with an average particle size value (D_{50}) of 4.012μm. Furthermore, the largest specific surface area (SSA) value was obtained at 222.9125 m^2/g with a similar treatment condition. Concerning the UFTRHA morphology, particle agglomeration was observed for samples with a grinding duration of more than 15 minutes. Therefore, grinding parameters involved in the process are proven to affect the physical and morphological attributes of UFTRHA produced. Particle size reduction and significant SSA value of UFTRHA are vital for effective pozzolanic reaction and hence promote a greater material performance as a superior additive in concrete application.

Keywords: Ultrafine treated rice husk ash (UFTRHA), Mechanical activation process, Morphology of UFTRHA, Particle size distribution, Specific surface

1. INTRODUCTION

The construction industry that adopts high-quality materials encourages engineers to find building technology innovations. For example, the concrete typically composed of Portland cement, fine aggregates, coarse aggregates, and mixed with water has delivered the need for high compressive strength material in this industry. However, the significant development of concrete also indirectly leads to the decline of environmental quality.

According to International Energy Agency (2015), the steel and cement industry was responsible for 8% and 15% of total global energy consumption and global anthropogenic carbon dioxide exposure in 2012. Consequently, the emissions hike from these sectors occurred rapidly over the 20 years [1].

According to BERNAS, a body responsible for Malaysia's domestic paddy and rice industry, this abundance by-product is usually used as biomass fuel for boilers for electricity generation within the factory area.

However, the rice husk generated is still underutilized at the factory. The problem becomes complicated when BERNAS removes the rice husk from the factory since this activity incurred extra costs for the company. Therefore, there is an urge to make use of this abundance by-product in the industries, namely the construction industry.

The major constituent of concrete is aggregate, which may be natural (gravel or crushed rock with sand) or artificial (blast furnace slag, broken brick, and steel shot). Another constituent is the binder, which is quite expensive but essential as it holds together the aggregate particles to form concrete [2].

In this regard, most researchers are currently working on using agricultural wastes as pozzolana to replace cement in concrete production. Pozzolana acts as a binder and reacts with calcium hydroxide ($Ca(OH)_2$) formed from the hydration process of cement. Therefore, the pozzolana is added to the cement mixture to promote concrete strength development.

Recently, natural pozzolans have been widely used in natural conditions or after calcination. These pozzolans act as void-filling particles between aggregates and cement paste, improve the rheological properties of concrete mix and the

production of secondary hydrates matrix product via pozzolanic reaction with $Ca(OH)_2$ or portlandite, which results from the primary hydration process of Portland cement and water.

Based on ASTM C-618-19 has outlined the fundamental requirements and classifications for coal fly ash and raw or calcined natural pozzolans, the total content of these three components, namely silicon dioxide (SiO_2), aluminum oxide (Al_2O_3) and iron oxide (Fe_2O_3) must be equivalent to 70% or more [3].

In light of incorporating rice husk ash (RHA) as an additive material into concrete production, it is regarded as one due to its high silica content [4]–[7]. Therefore, pozzolan can be used as a primary constituent of concrete in the construction industry. The absorbed silica is then eventually assimilated into its structure during the growth [8]. Thus, the outer part, which refers to rice husk, possesses high silica content with a value of more than 80% [8]. Furthermore, adding biomass-derived particles could act as a filler to improve the strength of the material [10]–[12].

Recently, there is extensive research on the incorporation of RHA in concrete has been done due to its high silica content. Despite the high number of experimental works done in this area since the 1970s, the quality of the RHA is still compromised. Unlike other types of material, such as fly ash and silica fume, this material is still not widely used as additive material among the construction key players. However, the research on the RHA has begun in the 1970s.

Among the reasons that hindered the utilization of RHA in the current construction industry are the inconsistency of its amorphousness degree with undesirable composition, i.e., potassium oxide (K_2O) and sodium oxide (Na_2O). These compositions cause pure silica content in the RHA to melt at low temperatures, i.e., less than 800°C [4, 13].

It is known as a eutectic reaction, where the metallic impurities encapsulating the husk's surface melt during the burning process and reduce the specific surface area of the burnt ash. Consequently, the pozzolanic reactivity of the ashes will be reduced. Therefore, using RHA in concrete is favorable for material cost reduction. Still, a study on the effect of mechanical activation via planetary ball mill on RHA has never been reported. The mechanical activation process significantly influences the behaviour of RHA [14].

Despite this fact, there is a need to investigate further the influence of mechanical activation via planetary ball mill on the quality enhancement of additive material production for concrete application from locally available agricultural waste since it is limited discussed by past researchers.

In this paper, mechanical activation is utilized as a feasible method to significantly reduce average particle size and eventually increase the specific surface area (SSA) in powder form. Therefore, this paper is focused on the mechanical activation process to produce ultrafine size (<5μm) of treated RHA to achieve optimum reaction of the material as a reactive additive in concrete production. It is expected that the reactive treated RHA enhances the quality of concrete produced and hencbenefitsit the civil engineering field.

2. RESEARCH SIGNIFICANCE

The study aims to identify the effect of using a planetary ball mill in the mechanical activation process as an essential process to produce high-quality ultrafine treated rice husk ash (UFTRHA). Then, finding the performance of concrete, i.e., pozzolanic activity, concrete durability, and interfacial transition zone (ITZ) characteristics in concrete to examine its suitability in producing reactive pozzolan.

Hence, it can reduce carbon dioxide emissions to the atmosphere. Sustainable practices, processes, and promotion of green materials in every economic and technological sector are currently considered the world's top plan to achieve via research.

3. EXPERIMENTAL METHOD

In this study, the raw rice husk (RH) is acquired from a single local rice milling plant (BERNAS) in Sungai Ranggam. At the same time, the acid used in the thermochemical pretreatment process is an analytical grade (AG) hydrochloric acid 37% (HCl) supplied by R & M Chemicals.

The raw RH undergoes the essential processes of thermochemical pretreatment, incineration, and mechanical activation to produce the ultrafine size of treated rice husk ash (UFTRHA).

The UFTRHA was produced at 600°C and pretreated with 0.1M hydrochloric acid (HCl) at 80°C for 4 hours of the soaking period will be examined in the grinding process. This is because it has the highest silicon dioxide (SiO_2) content, i.e., 98.6% from x-ray fluorescence (XRF) analysis.

4. RESULT AND DISCUSSIONS

4.1 Structural Elucidation of UFTRHA and NTRHA

Fourier transmission infrared spectroscopy (FTIR) testing exposed the functional groups of UFTRHA to the pretreatment process and various combustion variants. The NTRHA and UFTRHA samples were also examined for comparison accordingly. Fig.1 and Fig.2 illustrate the FTIR spectra of NTRHA and UFTRHA, respectively.

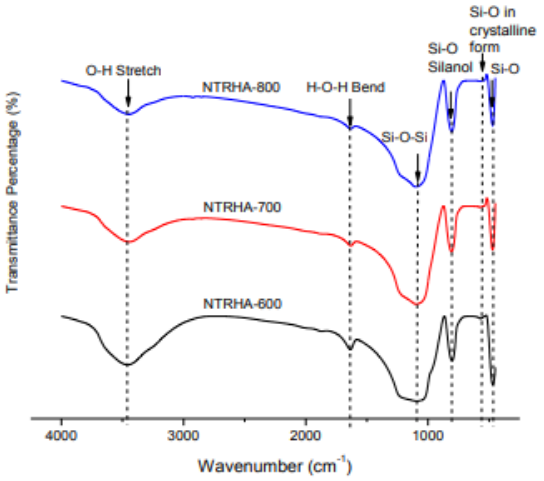

Fig.1 FTIR spectra of optimum NTRHA subjected to the different combustion temperature exposures

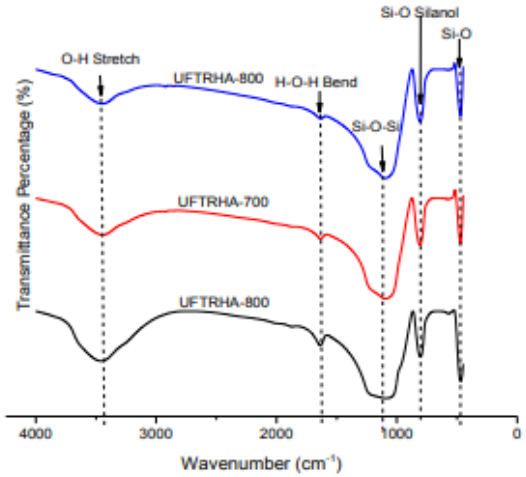

Fig.2 FTIR spectra of optimum UFTRHA subjected to the different combustion temperature exposures

As for NTRHA powder samples in Fig.1, transmittance percentage peaks corresponding to the Si-O element bond were observed at 472 to 475cm^{-1}, 620 to 621 cm^{-1}, and 800 to 803cm^{-1}. The transmittance peak at 472 to 475cm^{-1} was related to the Si-O rocking bond. Meanwhile, the peak at wavenumber in the 800 to 803cm^{-1} resembled the silanol symmetric bond vibration. But, the weak band from 620 to 621cm^{-1} was evidence of crystalline cristobalite formation in the silica phase in NTRHA [15], [16].

At the band signal 1103 to 1104 cm^{-1}, vibrational stretching of asymmetric Si-O-Si in SiO4 tetrahedron was detected. This was evidence of a stoichiometric SiO_2 structure [17]. The absorption bands at 3428 to 3445 cm^{-1} were assigned as O-H stretching bend modes of the adsorbed water.

On the other hand, UFTRHA samples subjected to different incineration temperatures, as shown in Fig.2, exhibited more or less like functional groups. Characteristics of NTRHA samples discussed previously. Like NTRHA samples, vibration bands at 471 to 475 cm^{-1}, 803 to 804 cm^{-1}, and 1099 to 1103 cm^{-1} were assigned to the Si-O rocking band, symmetric Si-O band as well as asymmetric stretching of Si-O-Si band, subsequently. These three peaks are a significant indication of silica material.

In addition, there was no signal peak detected around 620 cm^{-1} for all UFTRHA samples. This was a sign of amorphous silica formation in all UFTRHA samples. Meanwhile, the H-O-H bending and O-H stretching vibration modes were observed in the band area between 1629 to 1634 cm^{-1} and 3436 to 3447 cm^{-1}, respectively.

4.2 Physical Characteristics of UFTRHA and NTRHA

The laser particle size analysis was employed to find the grinding effect on the particle size distribution (PSD) of non-treated rice husk ash (NTRHA) and UFTRHA.

Table 1 PSD details of optimum UFTRHA-600°C ground with BPR value of 15:1 at various speeds and duration

Grinding speed (rpm)	Grinding duration (Min)	Particle size (µm)		
		D_{10}	D_{50}	D_{90}
-	-	3.251	15.973	53.973
100	15	1.444	5.383	18.469
	30	1.514	5.300	15.959
	45	1.483	5.289	17.574
	60	1.603	5.044	14.074
200	15	1.285	5.071	20.791
	30	1.250	5.074	21.975
	45	1.323	5.044	17.881
	60	1.325	5.027	16.618
300	15	0.598	4.012	15.735
	30	1.393	4.380	14.144
	45	1.295	4.473	15.254
	60	1.460	4.676	14.768

For PSD analysis, the most crucial information is D_{50}, as this value indicates the average particle size of the tested material in powder form. As shown in Table 1, the observed trend of the average particle size pattern for UFTRHA-600°C at a milling speed of 300rpm contradicted the other speeds of 100rpm and 200rpm.

The most crucial information from PSD analysis is D_{50}, as this value indicates the powder-forming average particle size of the tested material. Based on the results, it can be seen that the D_{50} value of

UFTRHA decreased as the grinding time and speed increased.

However, the UFTRHA-600℃ at 300rpm for about 15 minutes has the lowest D_{50} value. At only 15 minutes of the grinding period, the D_{50} value reduced dramatically from 15.973μm to 4.012μm.

Moreover, it is reported that the lowest value of D_{50} will reduce the average volume of pores, and this is because of the elimination of some pores due to the mechanical activation process [14]. In addition, the shearing impact between grinding media (balls) and feedstock (UFTRHA) occurs vigorously in the system hence the smaller particle size obtained within a short time. This is evident that long milling duration at high speeds leads to particle agglomeration through excessive grinding [17].

Compared to the UFTRHA-600 powder sample, NTRHA-600 ground at 0rpm to 300rpm possessed a relatively larger D_{50} value at the grinding duration of 15 minutes compared to UFTRHA-600 samples, as shown in Table 2. The specific PSD of UFTRHA can be achieved by either minimizing the grinding speed and escalating the grinding duration or vice versa, as reported elsewhere [19].

In addition, the UFTRHA-600℃ grain yielded had a smaller length than the NTRHA-600℃ ash. The metallic impurities present on the surface of the NTRHA caused the remaining carbon content in the NTRHA to be removed during the combustion process, hence defining the color difference. The trapped carbon content easily dissolved and remained in such ternary of Si–Na–O and Si–K–O oxides that melted on the surface of SiO_2 during the burning procedure [20].

Table 2 PSD details of optimum NTRHA-600℃ ground with BPR value of 15:1 at various speeds and duration

Grinding speed (rpm)	Particle size (μm)		
	D_{10}	D_{50}	D_{90}
-	3.213	28.002	194.82
100	1.115	7.807	26.17
200	1.442	5.951	24.471
300	1.339	5.158	18.704

Vankatanarayanan and Rangaraju [21] also mentioned that the NTRHA has a wide range of particle size distribution which needs to undergo a mechanical activation process to obtain finer particles with a consistent size and shape. Therefore, the high performance of ashes will be achieved.

From this analysis, the lowest D_{50} of UFTRHA-600℃ value was observed when a grinding speed of 300rpm for about 15 minutes, where at this speed and duration, ultrafine size particles were produced.

Therefore, at a BPR value of 15:1 and grinding speed of 300rpm, 15 minutes of the grinding period was sufficient. This phenomenon was due to the high speed of the grinding process, which resulted in greater velocity of the ball movements in the milling bowl. Therefore, the extended milling period was insignificant for particle size reduction purposes.

In conclusion, the lowest D_{50} of UFTRHA-600 value was observed by adopting a grinding speed of 300rpm, where at this speed, ultrafine size particles (<5μm) were successfully obtained.

4.3 Specific Surface Area (SSA) of UFTRHA and NTRHA

The mechanical grinding procedure indeed affects the porous structure of porous materials. In this regard, the specific surface area (SSA) and pore characteristics of the porous structure of NTRHA and UFTRHA were assessed using the Brunauer Emmet Teller (BET) and Barret Joyner Halenda (BJH) techniques.

The NTRHA and UFTRHA were prepared with various combustion temperatures at optimum grinding parameters (grinding at 300rpm speed with BPR 15:1 for 15 minutes). From Table 3, the SSA of NTRHA-600, NTRHA-700, and NTRHA-800 was recorded to be 4.8291, 40.3123, and 28.1305 m^2/g.

On the other hand, SSA values for UFTRHA-600, UFTRHA-700, and UFTRHA-800 were observed as 222.9125, 205.1350, and 219.5759 m^2/g, respectively. Furthermore, the result showed that UFTRHA-600 possessed the remarkably highest SSA value (222.9125 m^2/g) among the samples due to the smallest particle size (D_{50} = 4.012μm).

A massive difference in SSA values for both NTRHA and UFTRHA is shown in Table 3. This phenomenon was due to higher unburnt carbon content in NTRHA that increased rigidity to the NTRHA structure, making it a harder material to be milled. Van, Bui, and Ludwig [22] mentioned that NTRHA consists of macroporous (size of particles > 50 nm) and mesoporous (size of particles between 2 to 50 nm).

Then, the burnt sample's color seems dark due to the higher amount of unburnt carbon content. From Fig.3, it can be seen that UFTRHA formed white ashes meanwhile NTRHA produced grey-black ashes. Therefore, it can be said that a high amount of unburnt carbon causes difficulties in breaking the material into smaller particle sizes through the milling process.

In addition, one of the reasons that contributed

to the highest SSA value of UFTRHA-600 was due to the smallest particle size of this sample, as reported in the previous section, i.e., D_{50} is 4.012µm. However, based on the BJH evaluation of pore characteristics in Table 3, all UFTRHA samples were classified as mesoporous structured material since the average pore diameter recorded was less than 9 nm.

Table 3 Pore features and specific surface area (BET-SSA) of NTRHA and UFTRHA prepared with various combustion temperature

Samples	Specific surface area (BET-SSA) (m^2/g)	Pore features (BJH)		
		Adsorption cumulative pore surface area (m^2/g)	Adsorption cumulative pore volume (cm^3/g)	Adsorption cumulative average pore diameter (nm)
NTRHA-600	4.8291	3.9110	0.0201	30.5403
NTRHA-700	40.3132	34.2670	0.1456	12.5530
NTRHA-800	28.1305	25.5360	0.1075	22.8062
UFTRHA-600	222.9125	167.6350	0.2423	5.5593
UFTRHA-700	205.1350	151.2060	0.2330	6.2720
UFTRHA-800	219.5759	154.5550	0.2351	6.2203

Usually, the pore size distribution for the mesoporous structured materials had narrow range values, i.e., between 2 to 22 nm, with the average pore diameter value from 2 to 9 nm [17,18].

Overall, the mesoporous UFTRHA-600 with optimum grinding parameters was identified to have the highest SSA, pore surface area, pore volume, and lowest average pore diameter values. In addition, the more delicate ashes had a performance as a reactive mineral additive construction material than the coarser ashes [25].

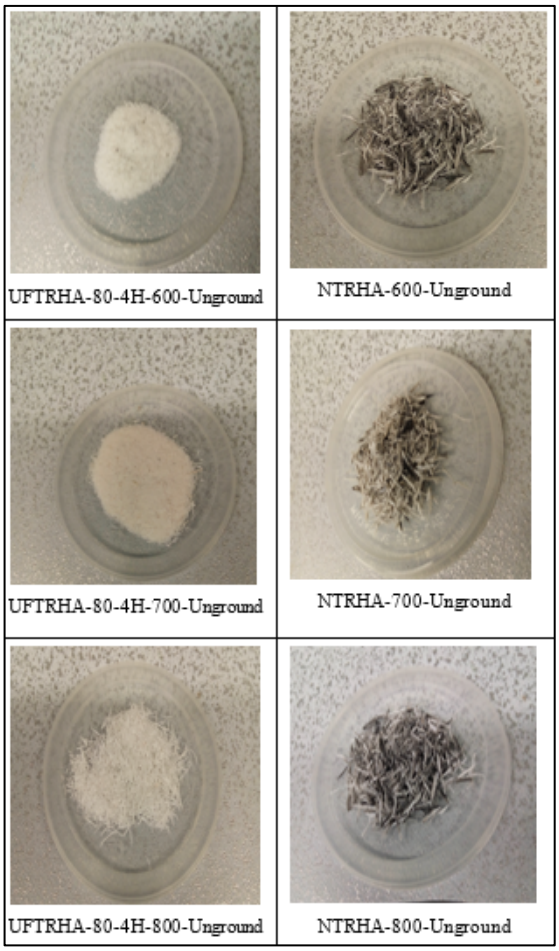

Fig.3 Digital photo of UFTRHA and NTRHA prepared at various combustion temperatures.

4.4 Morphology of UFTRHA and NTRHA

Based on the Field Emission Scanning Electron Microscopy (FESEM) image of NTRHA ash, as illustrated in Fig.4, it had a corrugated, rough surface, rigid structure with cone-shaped protuberances. The physical characteristics of NTRHA ash were similar to the condition of unground RHA prepared at 600°C reported by Xu, Lo, and Memon [26], where the RHA's outer surface is dense and looks like a net strip with arranged conical protrusion. In addition, the outer surface of NTRHA is highly corrugated and ridged.

Moreover, the high content of unburnt carbon also contributed to the rigidity of the NTRHA ash. Therefore, the presence of unburnt carbon is due to the burning process. On the other hand, the unground UFTRHA FESEM image in Fig.2

indicated the ash's soft structure. Therefore, it was evident that the structure was already broken into small pieces even though no grinding aid had been introduced to the ash powder.

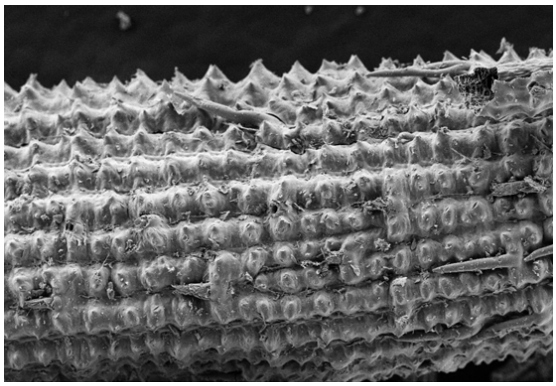

Fig.4 NTRHA-600 FESEM image captured 100X magnification

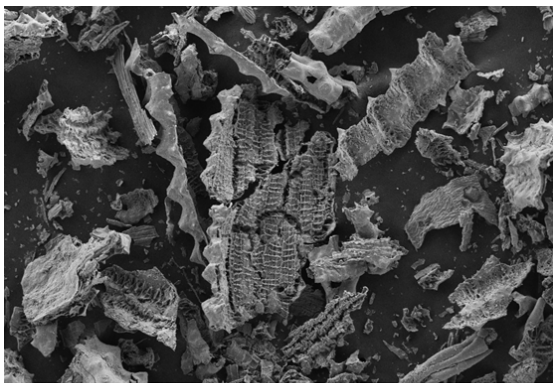

Fig.5 UFTRHA-600 FESEM image captured 100X magnification

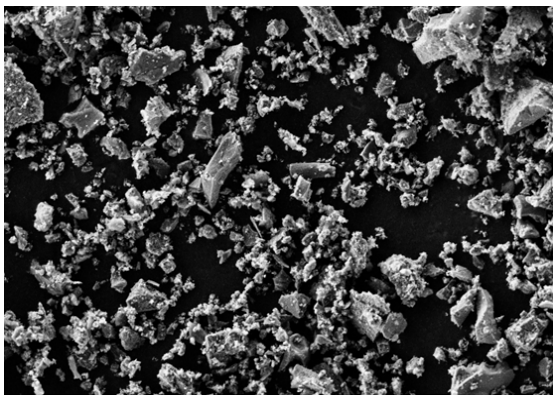

Fig.6 FESEM images of UFTRHA-600 ground for 15 minutes, with grinding speed of 300rpm and BPR value of 15:1

Based on Fig.5, the pore was already exposed, filled with agglomerated particles of UFTRHA finely even with no mechanical grinding imposed on the powder sample. This is due to the acid treatment process that successfully breaks the rigid structure of lignocellulosic materials. The rice husk's hemicellulose, cellulose, and lignin are examples of lignocellulosic materials.

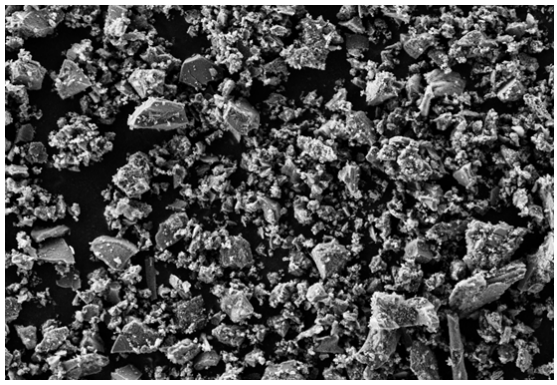

Fig.7 FESEM images of UFTRHA-600 ground for 30 minutes, with grinding speed of 300rpm and BPR value of 15:1

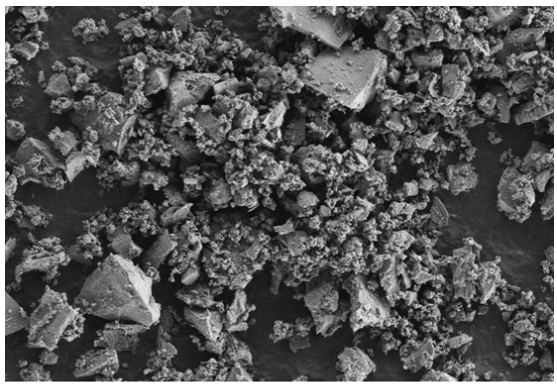

Fig.8 FESEM images of UFTRHA-600 ground for 45 minutes, with grinding speed of 300rpm and BPR value of 15:1

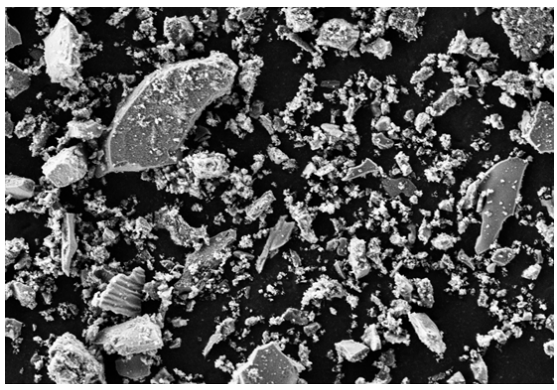

Fig.9 FESEM images of UFTRHA-600 ground for 60 minutes, with grinding speed of 300rpm and BPR value of 15:1

During the acid treatment process, the biomass hierarchy breakdown of the intermolecular and

intramolecular bonds in cellulose and hemicellulose of husk occurred and interrupted its rigid structure. A similar observation has also been reported by Lee, Hamid, and Zain [27].

To quantitatively analyze the effect of grinding duration on the morphology of UFTRHA in this study, the FESEM technique was used at a high magnification of 1000X. The morphologies of the UFTRHA particles for grinding duration variation (15, 30, 45, and 60 minutes) are shown in Fig.6 to 9.

5. CONCLUSIONS

In a nutshell, the mechanical activation process is proven effective in producing a highly reactive UFTRHA. The average particle size decreased with increases in both grinding speed and grinding duration for speeds of 100rpm and 200rpm. However, 300rpm for about 15 minutes of milling was sufficient to produce ultrafine particle size (<5μm) of ashes. As for BET-SSA analysis, UFTRHA-600^{o}C had the highest value of 222.9125m^2/g with the optimum grinding condition of 300rpm grinding speed for 15 minutes. The morphology of UFTRHA included the soft structure of the ash, which broke into small pieces, although no grinding aid has been introduced to the ash powder. As a result, the pores of UFTRHA are filled with agglomerated ash particles. Both UFTRHA and NTRHA powders had agglomerated particles with irregular shapes due to the high-energy milling effect. Thus, the extended grinding period (> 15 minutes) caused particle agglomeration. Hence, larger particle sizes and lower BET-SSA values were yielded. Lastly, it is suggested to investigate further the effect of UFTRHA in other characterization properties of ash, such as x-ray diffraction (XRD) analysis and transmission electron microscopy (TEM) analysis. Also, the expansion of this research work by incorporating UFTRHA in concrete is strongly recommended for further investigation of its mechanical properties accordingly.

6. ACKNOWLEDGMENTS

The author would like to express the highest gratitude to the Ministry of Higher Education Malaysia (MoHE) under Fundamental Research Grant Scheme, project ID FRGS19-171-0780 for funding this research.

7. REFERENCES

[1] Van Ruijven B. J., Van Vuuren D. P., Boskaljon W., Neelis M. L., Saygin D., and Patel M. K., “Long-term model-based projections of energy use and CO_2 emissions from the global steel and cement industries,” Resour. Conserv. Recycl., vol. 112, pp. 15–36, 2016, doi: 10.1016/j.resconrec.2016.04.016.

[2] Krauss P. and Paret T., "Review of Properties of Concrete," J. Perform. Constr. Facil., vol. 28, no. 3, pp. 630–630, 2014, doi: 10.1061/(asce)cf.1943-5509.0000595.

[3] ASTM C 618-19, "Standard Specification for Coal Fly Ash and Raw or Calcined Natural Pozzolan for Use in Concrete," ASTM Int., pp. 1–5, 2019, doi: 10.1520/C0618-19.

[4] Xu W., Wei J., Chen J., Zhang B., Xu P., Ren J. and Yu Q., "Comparative study of water-leaching and acid-leaching pretreatment on the thermal stability and reactivity of biomass silica for viability as a pozzolanic additive in cement," Materials (Basel)., vol. 11, no. 9, 2018, doi: 10.3390/ma11091697.

[5] Jittin V., Bahurudeen A., and Ajinkya S. D., "Utilisation of rice husk ash for cleaner production of different construction products," J. Clean. Prod., vol. 263, p. 121578, 2020, doi: 10.1016/j.jclepro.2020.121578.

[6] Nayak P. P. and Datta A. K., "Synthesis of SiO_2-Nanoparticles from Rice Husk Ash and its Comparison with Commercial Amorphous Silica through Material Characterization," Silicon, vol. 13, no. 4, pp. 1209–1214, 2021, doi: 10.1007/s12633-020-00509-y.

[7] Isberto C. D., Labra K. L., Landicho J. M B., and De Jesus R., "Optimized preparation of rice husk ash (RHA) as a supplementary cementitious material," Int. J. GEOMATE, vol. 16, no. 57, pp. 56-61, 2019, doi:10.21660/2019.57.4628.

[8] Cornelis J. T., Titeux H., Ranger J., and Delvaux B., "Identification and distribution of the readily soluble silicon pool in a temperate forest soil below three distinct tree species," Plant Soil, vol. 342, no. 1–2, pp. 369–378, 2011, doi: 10.1007/s11104-010-0702-x.

[9] Rodrigues F. A. and Datnoff L. E., "Silicon and plant diseases," Silicon Plant Dis., pp. 1–148, 2015, doi: 10.1007/978-3-319-22930-0.

[10] Fathana H., Iqhrammullah M., Rahmi R., Adlim M., and Lubis S., "Tofu wastewater-derived amino acids identification using LC-MS/MS and their uses in the modification of chitosan/TiO_2 film composite," Chem. Data Collect., vol. 35, no. March, p. 100754, 2021, doi: 10.1016/j.cdc.2021.100754.

[11] Rahmi, Lubis S., Az-Zahra N., Puspita K., and Iqhrammullah M., "Synergetic photocatalytic and adsorptive removals of metanil yellow using TiO_2/grass-derived cellulose/chitosan film composite," Int. J. Eng. Trans. B Appl., vol. 34, no. 8, pp. 1827–1836, 2021, doi: 10.5829/ije.2021.34.08b.03.

[12] Iqhrammullah M., Marlina, Hedwid R.,

Karnadi I., Kurniawan K. H., Olaiya N. G., Mohamad Hafiz M. K., Abdul Khalil H. P. S., and Abdulmadjid S. N., "Filler-modified castor oil-based polyurethane foam for the removal of aqueous heavy metals detected using laser-induced breakdown spectroscopy (LIBS) technique," Polymers (Basel)., vol. 12, no. 4, 2020, doi: 10.3390/POLYM12040903.

[13] Bazargan A., Bazargan M., and McKay G., "Optimization of rice husk pretreatment for energy production," Renew. Energy, vol. 77, pp. 512–520, 2015, doi: 10.1016/j.renene.2014.11.072.

[14] Vieira A. P., Toledo F. R. D., Tavares L. M., and Cordeiro G. C., "Effect of particle size, porous structure and content of rice husk ash on the hydration process and compressive strength evolution of concrete," Constr. Build. Mater., vol. 236, p. 117553, 2020, doi: 10.1016/j.conbuildmat.2019.117553.

[15] Lee T., Othman R., and Yeoh F. Y., "Development of photoluminescent glass derived from rice husk," Biomass and Bioenergy, vol. 59, no. September, pp. 380–392, 2013, doi: 10.1016/j.biombioe.2013.08.028.

[16] Roy S., Das P., and Sengupta S., "Treatability study using novel activated carbon prepared from rice husk: Column study, optimization using response surface methodology and mathematical modeling," Process Saf. Environ. Prot., vol. 105, pp. 184–193, 2017, doi: 10.1016/j.psep.2016.11.007.

[17] Sankar S., Sharma S. K., Kaur N., Lee B., Kim D. Y., and Lee S., Jung H., "Biogenerated silica nanoparticles synthesized from sticky, red, and brown rice husk ashes by a chemical method," Ceram. Int., vol. 42, no. 4, pp. 4875–4885, 2016, doi: 10.1016/j.ceramint.2015.11.172.

[18] Xu W., Lo Y. T., Ouyang D., Memon S. A., Xing F., Wang W., and Yuan X., "Effect of rice husk ash fineness on porosity and hydration reaction of blended cement paste," Constr. Build. Mater., vol. 89, pp. 90–101, 2015, doi: 10.1016/j.conbuildmat.2015.04.030.

[19] Venkatanarayanan H. K. and Rangaraju P. R., "Material Characterization Studies on Low- and High-Carbon Rice Husk Ash and Their Performance in Portland Cement Mixtures," Adv. Civ. Eng. Mater., vol. 2, no. 1, p. 20120056, 2013, doi: 10.1520/acem20120056.

[20] Umeda J. and Kondoh K., "High-purification of amorphous silica originated from rice husks by a combination of polysaccharide hydrolysis and metallic impurities removal," Ind. Crops Prod., vol. 32, no. 3, pp. 539–544, 2010, doi: 10.1016/j.indcrop.2010.07.002.

[21] Venkatanarayanan H. K. and P. R. Rangaraju, "Effect of grinding of low-carbon rice husk ash on the microstructure and performance properties of blended cement concrete," Cem. Concr. Compos., vol. 55, pp. 348–363, 2015, doi: 10.1016/j.cemconcomp.2014.09.021.

[22] Van V. T., Rößler C., Bui D. D., and Ludwig H. M., "Mesoporous structure and pozzolanic reactivity of rice husk ash in the cementitious system," Constr. Build. Mater., vol. 43, pp. 208–216, 2013, doi: 10.1016/j.conbuildmat.2013.02.004.

[23] Wang W., Martin J. C., Fan X., Han A., Luo Z., and Sun L., "Silica nanoparticles and frameworks from rice husk biomass," ACS Appl. Mater. Interfaces, vol. 4, no. 2, pp. 977–981, 2012, doi: 10.1021/am201619u.

[24] Alothman Z. A., "A review: Fundamental aspects of silicate mesoporous materials," Materials (Basel)., vol. 5, no. 12, pp. 2874–2902, 2012, doi: 10.3390/ma5122874.

[25] Ahsan M. B. and Hossain Z., "Supplemental use of rice husk ash (RHA) as a cementitious material in the concrete industry," Constr. Build. Mater., vol. 178, pp. 1–9, 2018, doi: 10.1016/j.conbuildmat.2018.05.101.

[26] Xu W., Lo T. Y., and Memon S. A., "Microstructure and reactivity of rice husk ash," Constr. Build. Mater., vol. 29, pp. 541–547, 2012, doi: 10.1016/j.conbuildmat.2011.11.005.

[27] Lee H. V., Hamid S. B. A., and Zain S. K., "Conversion of lignocellulosic biomass to nanocellulose: Structure and chemical process," Sci. World J., vol. 2014, 2014, doi: 10.1155/2014/631013.